ELSEVIER

PII:S0958-9465(96)00021-1

Cement and Concrete Composites 18 (1996) 281–297

0958-9465/96/$15.00

Toughness Measurement — the Need to Think Again

B. Barr,[a] R. Gettu,[b] S. K. A. Al-Oraimi[a] & L. S. Bryars[a]

[a]Division of Civil Engineering, Cardiff School of Engineering, University of Wales Cardiff, Cardiff, UK
[b]Structural Technology Laboratory, Universitat Politècnica de Catalunya, Barcelona, Spain

Abstract

The first part of the paper reviews a number of concurrent developments which have taken place in recent years in the concrete research area. The developments include the commercial development of FRC materials, the proposals for evaluating the enhanced performance of FRC materials, the development of high performance (high strength/brittle) concretes, the application of fracture mechanics to concrete together with the revolution in testing machines with the introduction of closed-loop testing. The limitations of current standards and guidelines for evaluating the toughness of FRC materials are also reviewed and proposals for overcoming these limitations are advanced. It is proposed that notched beams, subjected to three-point loading, rather than unnotched beams subjected to four-point loading should be used for toughness measurement and that the deformation of the beams should be measured directly from the specimen rather than through the testing machine. © 1996 Elsevier Science Limited.

INTRODUCTION

During the last thirty years (1960s – 90s) fibre reinforced cements and concretes (FRC) have developed progressively and today a range of fibres and similar products are commercially available.[1–3] In parallel with the commercial development of FRC materials an extensive research programme has been undertaken to quantify the enhanced properties of FRC materials and, in particular, to allow comparisons to be made between various fibres. The enhanced toughness and impact resistance of FRC materials, relative to plain concrete, are two properties which have received considerable attention, although FRC materials also exhibit improved fracture and fatigue characteristics. Whereas impact tests readily demonstrate the enhanced properties of FRC materials, such tests require sophisticated equipment and instrumentation. Consequently, tests which allow the toughness of FRC materials to be measured have received the greatest attention.

Toughness is not the easiest of terms to define and its measurement has been a source of argument during the last twenty years. In general terms, the toughness of FRC materials can be considered as their energy absorption capacity which is conventionally characterised by the area under the load–displacement curve obtained experimentally. Although a range of tests has been carried out on FRC materials (including tension, compression, shear and torsion) most toughness measurements have been performed on unnotched beams in flexure using a four-point loading arrangement. A review of the general features and methods of interpretation of results from four-point loading tests has been given recently by Gopalaratnam and Gettu.[4] The review describes the use of various toughness measurements (energy-based dimensionless indices, energy absorption capacity, strength-based dimensionless indices, residual strength indices, equivalent flexural strength and deflection-based dimensional indices) in European, American and Japanese standards.

A review of the early development of energy-based dimensionless toughness indices has been given elsewhere[5] and will not be repeated in detail here. Essentially the practical application of this method began with the introduction of the ACI 544 Toughness Index,[6] based on the work of Henegar.[7] ACI Committee 544 defined the toughness index as the ratio of the amount of energy required to deflect a fibre concrete beam by a prescribed amount to the energy required to bring the fibre beam to the point of first crack (Fig. 1(a)). Similar notions were used in the development of the ASTM C 1018 standard,[8] based on the work of Johnston.[9] The main improvement in the ASTM C 1018 standard compared with the ACI 544 recommendation is that toughness indices (I_5, I_{10}, etc.) are determined for a number of prescribed deflections based on multiples of the first-crack

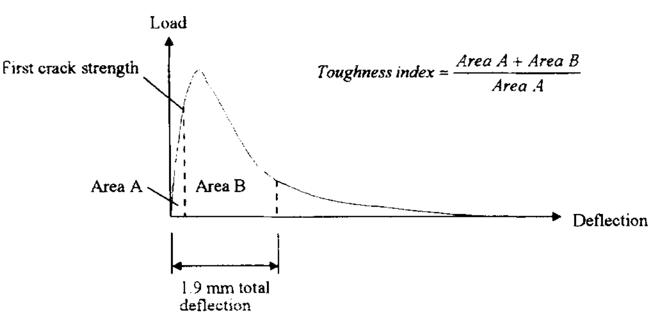

Fig. 1. (a). ACI Committee 544 toughness index.

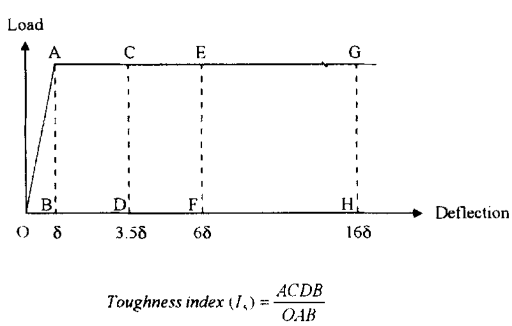

Fig. 1. (b). ASTM C 1018 toughness indices.

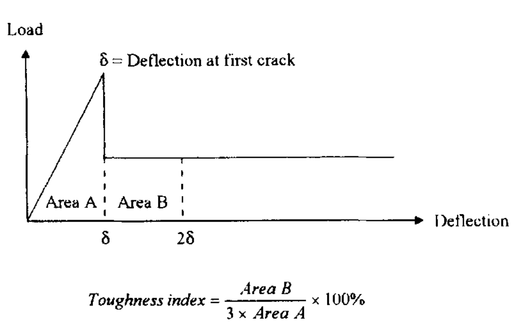

Fig. 1. (c). B/3A toughness index proposed by Barr and Hasso.[5]

deflection (Fig. 1(b)). The toughness index proposed independently by Barr and Liu[10] is similar to that of the Johnston/ACI 544 proposals in that it is based on the ratio of two areas under the load–deflection curve up to two-times the deflection at first-crack. The original definition of toughness index proposed by Barr and Liu was subsequently changed by Barr and Hasso [5] to that illustrated in Fig. 1(c). An important difference is that this particular toughness index was proposed for and has been applied to both notched and unnotched specimens subjected to various loading arrangements.

Significant developments are currently taking place in the development of high performance concretes. The use of high-strength silica fume concretes is continually increasing in scope and volume. Such materials follow the general trend in materials whereby increasing strength is accompanied by increasing brittleness. High strength brittle concrete is more prone to sudden catastrophic fracture than normal strength concretes. The simplest method of enhancing the toughness in such materials is by the inclusion of fibres in the matrix. The performance of high strength fibre reinforced materials can only be fully described by the use of both strength and toughness parameters.

The developments in high performance concretes during the last decade have occurred at the same time as a rapid expansion in the application of fracture mechanics to concrete. Currently three test methods for evaluating the fracture characteristics of plain concrete have emerged as potential standard test methods. RILEM Technical Committee 50-FMC[11] has proposed, based on the work of Hillerborg,[12] that the fracture energy of concrete, G_F, be determined via stable bend tests carried out on centrally notched beam specimens. In the G_F test the actual deflection of the beam is recorded rather than the displacement recorded by the testing machine. More recently, two further RILEM Draft Recommendations for fracture tests on concrete have been issued; one is based on the Size Effect Method and the other on the Two Parameter Method. The Size Effect Method[13] requires simply measuring the maximum loads in geometrically similar notched specimens of different sizes. The Two Parameter Method[14] considers cracking to be governed by the two parameters of critical stress intensity factor and the critical crack tip opening displacement ($CTOD_c$). The $CTOD_c$ is calculated from the crack opening that is measured directly off the test specimen. Some of the notions prevalent within the concrete fracture community (e.g. taking measurements directly from the test specimen) have influenced the concepts described herein, as reported later.

Also concurrently with the introduction of FRC materials, there has been a revolution in the methods of testing concrete in research laboratories. The 1960s saw the introduction of stiff testing machines to replace the old load-controlled machines. During the last ten years many laboratories have been using closed-loop servo-hydraulic machines to test concrete specimens in fracture tests. In such machines the opening of the crack mouth is used to control the test. In such tests, the crack mouth opening displacement (CMOD) can be used directly as a measure of the response of the beam, thus eliminating the need to monitor the actual central deflection of the test specimen. In view of the current developments in the testing of concrete, it is timely to reconsider the appropriateness of current notions and standards for evaluating the toughness of FRC materials.

CURRENT TOUGHNESS MEASUREMENTS

Most standards/guidelines[4] recommend the use of unnotched beam specimens subjected to four-point loading and the recording of net deflection at midspan is prescribed in most cases. The use of stiff testing machines, so as to achieve a prescribed rate of specimen deflection, is usually specified and a continuous load–deflection curve is required. Some variation in the size of the cross-section is accommodated by the standards (150×150 mm, 100×100 mm and shallower specimens for sprayed fibre concrete) depending on the type of fibre used. Although the general testing procedures are similar in the various standards, there are considerable variations in the methods used to interpret the results.

Perhaps the most widely reported toughness standard is the ASTM C 1018 standard (8) which is illustrated in Fig. 1(b). The first step in the use of this standard involves the determination of the first-crack, δ_f, which is often more difficult than that suggested by the schematic figure in Fig. 1(b). The standard defines the first-crack as 'the point of the load–deflection curve at which the form of the curve first becomes non-linear'. The accuracy of the recording system, the advent of micro-cracking and human judgement all influence the location of the point of first-crack. Having located δ_f, a number of toughness indices (I_5, I_{10} and I_{20}) can be evaluated corresponding to various portions of the post-first-crack curves being considered. The various portions of the load–deflection response are determined by multiples of the first-crack deflection; I_5 corresponding to 3.5 δ_f, I_{10} corresponding to 5.5 δ_f and I_{20} corresponding to 10.5 δ_f. (The subscripts 5, 10 and 20 are used since an elastic–plastic response would yield toughness indices with these values).

The ASTM C 1018 standard also requires the determination of dimensionless residual strength indices, in addition to the toughness indices. The residual strength indices provide an indication of the average strength sustained by the FRC beam whilst the beams are deflected from 3.5 δ_f to 5.5 δ_f ($R_{5,10}$) and from 5.5 δ_f to 15.5 δ_f ($R_{10,20}$). The limitations of these residual strength indices have been discussed in Ref. 4 and are not repeated here.

Some of the limitations of the ASTM C 1018 standard were identified by Gopalaratnam *et al.*[15] in their report of a round-robin test programme and by Banthia *et al.*[16] in their study of steel fibre reinforced dry-mix shotcrete. A frame (referred to as a 'yoke') was attached to their flexural beam specimens which allowed direct measurement of the net central deflection of the beam, i.e. the deflection was measured as that between the neutral axis of the beam and the top of the beam. The use of the 'yoke' eliminated extraneous deflections arising from support settlements and resulted in load–deflection curves which were significantly different from those observed by using the cross-head displacement of the testing machine. According to Banthia *et al.*,[16] it is only by using a 'yoke' arrangement that the real deflection can be determined and the apparent cross-head deflections are significantly in excess of theoretical deflections. The problems associated with the current definitions of toughness indices, as described by Banthia *et al.*,[16] can be overcome by combining the notion of toughness indices with tests on notched specimens used extensively by the concrete fracture community, as described below.

PROPOSED CRITERIA FOR TOUGHNESS MEASURES

Some of the views expressed by the authors here are based on their experience as members of the concrete fracture community. It is of interest to note the attitude of those working with FRC materials and those working on the fracture of concrete towards the need for standards. As reported above, Gopalartanam and Gettu[4] have compiled a summary of the essential features of thirteen standards already in use by the FRC community in Europe, North America and Japan. On the other hand, in the case of the fracture of concrete, three RILEM Draft Recommendations are still under consideration as possible standards, although they were proposed in 1985 (for the G_F test[11]), in 1990 (for the Size Effect Method[13]) and also in 1990 (for the Two Parameter Method[14]). The delay in introducing a standard test method for evaluating the fracture characteristics of concrete reflects the lack of interest by practising engineers in this topic. However, the situation is quite different in the case of FRC standards where practising engineers, as well as researchers, have made extensive use of standards.

The development of existing FRC standards and the introduction of new ones should ensure sufficient flexibility to satisfy the needs of research workers and practising engineers. At the present time, the existing standards are probably of greater interest to the research worker. This situation is perfectly acceptable since testing for comparison purposes between existing fibres, assessment of new fibres, assessment of influence of fibre volume and length, etc. is carried out in research laboratories. Nevertheless, taking a longer term view of standards, it is important to ensure that standards are capable of being used by practising engineers involved in the assessment of existing structures containing fibres. Structural assessment is often accompanied by taking cores from existing structures and hence some thought should be given to the possible use of cylindrical test specimen geometries.

Current standards for the evaluation of the toughness of FRC materials have a number of limitations. The main limitations include:

A range of parameters (energy-based dimensionless indices, energy absorption, residual strength indices, etc.) have been used to interpret test results gained from flexural tests. There is a need for consensus on the most appropriate parameter.

Beams have generally been tested in four-point bending resulting in greater variation in the recorded deflections compared with results gained from three-point bending.

The location of first crack is difficult to determine in many cases. The use of peak load to locate the position of first-crack would be an improvement.

Deflections have traditionally been recorded via the testing machine. These deflections significantly overestimate the actual net central deflection of the beam relative to its neutral axis. A number of improvements in deflection measurements have taken place in recent years, as described above.

The residual strength factors recommended in some standards have been shown to be unreliable.[17–19]

As in all other tests involving the fracture of concrete, the tests recommended in standards are subject to size effects.

Further details regarding the limitations of current standards are given in Ref 4.

Many of the limitations described above can be overcome by making the following adjustments to current standards:

Notched beams, subjected to three-point loading, as proposed in the G_F test recommendation should be used rather than unnotched beams, subjected to four-point loading. Other notched test specimens such as notched tension specimens should also be considered as possible test specimens.

The deformation of the beams should be measured directly from the test specimen rather than through the testing machine. This could be achieved readily by recording the crack mouth opening displacement (CMOD) rather than the net central deflection via a 'yoke' arrangement.

Some experimental work has already been carried out along the lines suggested above. Gopalaratnam *et al.*[17,18] proposed the use of notched beams, tested under servo-controlled conditions, to characterise toughness of FRC materials. In this study, the toughness was evaluated by means of the net central deflection, as given in ASTM C 1018. More recently, Bryars *et al.*[20,21] tested centrally loaded notched beams of steel fibre reinforced high strength concrete in which the toughness index was defined as the ratio between the areas under the load-CMOD curve until a prescribed multiple of the first-crack and until the first-crack. The experimental work reported here is an extension of the work reported in Refs 20 and 21.

EXPERIMENTAL CHARACTERIZATION OF TOUGHNESS USING NOTCHED SPECIMENS

Crack propagation and the associated material behaviour are best studied using notched specimens. This approach reduces the bulk energy dissipation and focuses the test on the behaviour of the material at and around the crack-tip. Such tests are especially important for materials that are weak in tension and are prone to brittle catastrophic failure, such as cement mortars and concretes. Notched specimens are also routinely used for characterizing fiber-reinforced composites and ceramics, mainly for quantifying the toughening due to the incorporation of fibres. The data from these tests is normally analysed using the concepts of fracture mechanics, the science of crack initiation and propagation. As mentioned earlier, several test procedures based on notched specimens have recently been proposed for characterizing the toughness of FRC.

Toughness characterization of plain concrete based on fracture mechanics

Since the failure of concrete is usually governed by crack propagation, fracture mechanics is a rational tool for characterizing its toughness. Consequently, several nonlinear fracture mechanics methods have been developed and validated for concrete. Though these approaches have mainly been applied to plain concrete, their consideration is relevant for the discussion of FRC for two important reasons: (i) the knowledge of the failure characteristics of the matrix (i.e. plain concrete) is essential for the analysis of the composite (i.e. FRC), and (ii) the properties of the plain concrete serve as references for quantifying any improvement due to the incorporation of fibres.

Most fracture mechanics based test methods use notched beams, where the crack initiates at the notch-tip and propagates along the notch plane. In order to obtain behaviour that is representative of the material, the dimensions of the beam, including the notch and unnotched ligament lengths, should be much larger, by at least three times that of the size of the largest inhomogeneity in the concrete. Also, some of these methods require that the crack opening (CMOD) be monitored and used to control the test.

Parameters based on the load–deflection curve of a notched specimen

One popular approach for quantifying the toughness of concrete is through the work-of-fracture. This concept is similar to those of several FRC toughness indices. The work-of-fracture is the energy required to break a specimen completely, which in a fracture test, corresponds to the area under the load vs load-point–displacement curve. The work-of-fracture for unit crack width and unit crack extension is called the fracture energy. The RILEM Draft Recommendation[11] for determining the fracture energy (G_F) of concrete requires the testing of a single-edge-notched center-loaded beam up to complete failure. Though G_F depends on the specimen size and notch depth, it can be considered, for practical purposes, as a measure of the energy absorbed during the failure of the concrete, as long as a standard specimen is used. Another parameter that is based on G_F is the characteristic length l_{ch} proposed by Hillerborg.[22] It is defined as G_F/Ef_t^2 (where E is the modulus of elasticity and f_t is the tensile strength) and is related to the size of the zone in which energy is dissipated during crack propagation. Therefore, l_{ch} is a measure of the ductility of the material. Typical values for l_{ch} are:[22,25] 5–15 mm for hardened cement paste, 100–200 mm for mortar, 200–500 mm for normal concrete, 0.5–3 m for glass fibre reinforced mortar, and 2–20 m for steel fibre reinforced concrete.

Parameters based on the pre-peak response of a notched specimen

Two RILEM Draft Recommendations for determining the fracture parameters of concrete[13,14] are based on the pre-peak nonlinearity exhibited by notched center-loaded beams. The Two Parameter Model of Shah uses the unloading compliance at the peak to determine the fracture toughness (K_{Ic}) and the critical crack-tip opening ($CTOD_c$). The Size Effect Method of Bazant[23] uses the peak loads of three different sizes of geometrically similar beams to obtain K_{Ic} and c_f, which is the effective size of the fracture process zone (i.e. the zone where energy is dissipated during crack propagation). Both these effective crack models describe the fracture of concrete with two parameters: one that reflects the resistance against cracking, K_{Ic}, and another related to the deformation or size of the fracture process zone, $CTOD_c$ or c_f. Accordingly, the latter set of parameters are considered to be measures of the toughening or the ductility of the concrete.[24,25] The basis for these models is linear elastic fracture mechanics, which governs crack propagation in ideal-brittle materials where the process zone is negligible.

EXTENSION OF FRACTURE BASED METHODS TO FIBRE-REINFORCED CONCRETES

Materials and tests used in the study

Medium strength concretes (MSC) series

The first series (denoted as MSC) consisted of tests on medium-strength concretes. Eight mixes were used: one plain concrete, three steel fibre reinforced concretes (with volume fractions, V_f, of 1%, 2% and 3%) and four polypropylene fibre reinforced concretes (with V_f of 0.1%, 0.2%, 0.3% and 0.4%). The base concrete had a cement:sand:gravel:water composition of 1:1.8:2.8:0.5, with portland cement, sea-dredged sand and crushed limestone gravel (maximum aggregate size = 10 mm). The fibres that were incorporated in the base concrete were National Standard Company steel fibres of 40 mm length and 0.4 mm diameter, and fibrillated polypropylene fibres of 50 mm length and 12000 denier (750 m/kg). Nine beams with dimensions of 100 × 100 × 500 mm and three 100 mm cubes were cast from each mix. Notches of 30, 40 and 50 mm length were cut with a masonry saw in six of the beams (two for each notch length). The notched beams were tested under three-point bending in a 250 kN closed-loop servo-hydraulic Schenck machine under crack opening (CMOD) control at a constant rate of 0.0375 mm/min. A clip gage was mounted across the notch mouth to monitor the CMOD. The deflection was measured using a transducer (LVDT) fixed to a rigid yoke (see Fig. 2) in order to eliminate the spurious effects due to local deformations at the supports. The unnotched beams were tested under three-point bending at the constant loading rate of 0.075 kN/min in a 600 kN closed-loop servo-hydraulic Avery–Denison machine to obtain the flexural strengths of the concretes. The cubes were tested in a Contest G.D. 10/250 machine to determine their compressive strengths. All the tests were performed at the age of 28 days. The compressive and flexural strengths for the different concretes are given in Table 1. It is observed, as expected, that the compressive strength is decreased marginally by the inclusion of polypropylene fibres (up to V_f = 0.3%) and increased marginally by the inclusion of steel fibres. A similar trend is observed in the case of the flexural strength results.

Typical load–deflection curves of the different concretes in the MSC series are shown in

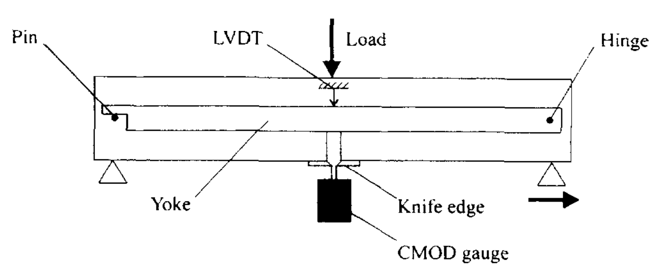

Fig. 2. Specimen and test setup used in the MSC series.

Table 1. Compressive and flexural strengths of concretes in MSC series

Concrete	V_f%		Compressive strength		Flexural strength	
	Steel	*Polypropylene*	*Average (MPa)*	*Variation (%)*	*Average (MPa)*	*Variation (%)*
MSC-0.0	0	0	49.7	1.5	8.13	5.2
MSCP-0.1	0	0.1	50.0	1.8	8.80	4.2
MSCP-0.2	0	0.2	48.8	3.3	7.76	2.8
MSCP-0.3	0	0.3	48.5	1.0	7.99	4.3
MSCP-0.4	0	0.4	43.5	4.0	7.08	3.7
MSCS-1.0	1	0	51.5	1.0	9.08	0.6
MSCS-2.0	2	0	52.0	1.9	8.75	5.1
MSCS-3.0	3	0	53.3	1.4	9.55	3.5

Figs 3–5. One obvious fact is that plain concrete exhibits a stable post-peak load–deflection response, which is contrary to the sudden drop in load assumed by several standards. It must be noted that when the test is controlled properly, plain concrete does exhibit some post-peak 'toughness'. The complete load–deflection curve of the plain concrete was used to determine the fracture energy G_F according to the RILEM recommendation based on the work-of-fracture.[11] The average value obtained for G_F is 108.3 N/m, with a coefficient of variation of 8.2%. Further details of the MSC series are given in the doctoral thesis of Al-Oraimi[26] and typical results are given in Table 2.

High strength concretes (HSC) series

The second series (denoted as HSC) consisted of tests on high strength concretes with and without steel fibres. The base concrete had the proportions of cement:sand:gravel:microsilica:water as 1:1.32:2.2:0.1:0.35, by weight. The cement was a Spanish type I-55A (similar to ASTM Type III and British type RHPC), the sand (0–5 mm) and gravel (5–12 mm) were crushed limestone, and the microsilica was a silica fume slurry (GRACE Force 10,000). 40 kg/m^3 ($V_f = 0.5\%$ approximately) of straight brass-coated high-strength steel BEKAERT OL6/.15 (0.15 mm diameter, 6 mm length) and OL13/.15 (0.15 mm diameter, 13 mm length) fibres were incorporated in this concrete. The plain concrete is denoted hereafter as HSC-0, and the fibres with the 6 mm and 13 mm fibres as HSC-6 and HSC-13, respectively. Different volumes of superplasticizer (GRACE Daracem 120, with 33% dry material and 67% water) had to be used to compensate the loss of workability due to the addition of the fibres (see Table 3). The slump obtained for each concrete is also given in Table 3. The inverted cone test could not be

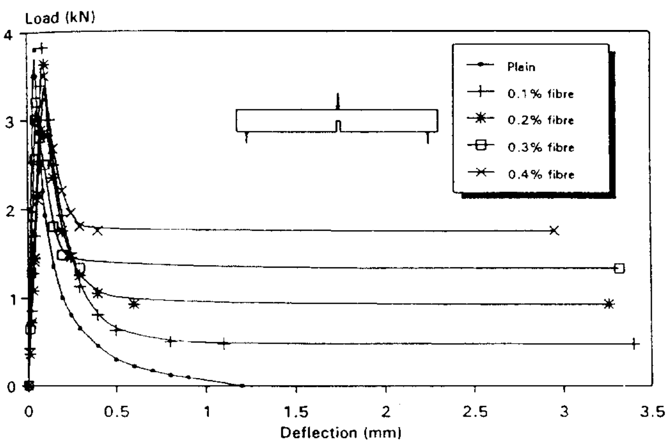

(a)Polypropylene fibre results

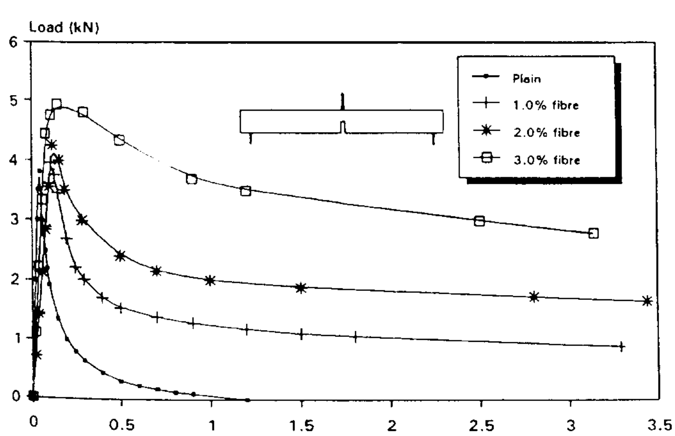

(b)Steel fibre results

Fig. 3. Load–deflection of beams with 30 mm notches; (a) polypropylene fibre concretes and (b) steel fibre concretes.

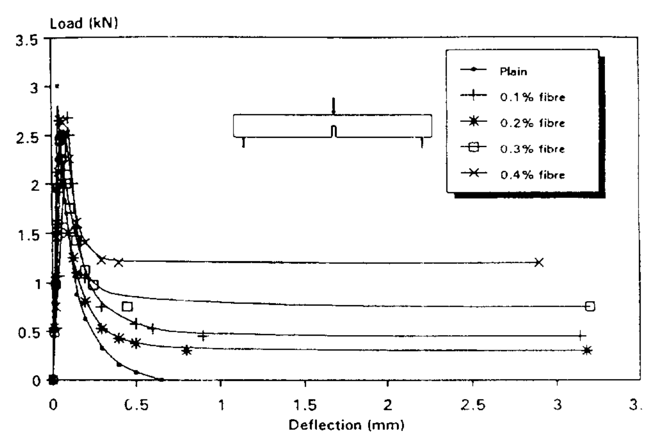

(a)Polypropylene fibre results

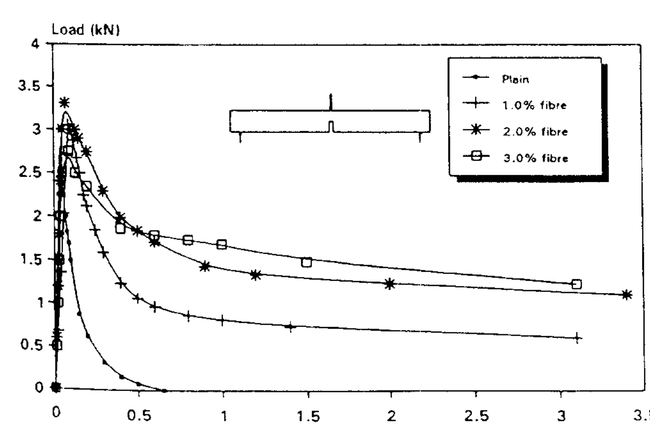

(b)Steel fibre results

Fig. 4. Load–deflection of beams with 40 mm notches; (a) polypropylene fibre concretes and (b) steel fibre concretes.

used for characterizing the workability due to the high fluidity of the concretes.

From each of the concretes, three 150×300 mm cylinders, three 100 mm cubes, three beams each with dimensions of $250 \times 80 \times 50$ mm, $500 \times 160 \times 50$ mm and $1000 \times 320 \times 50$ mm, and three panels each with dimensions of $60 \times 75 \times 50$ mm, $120 \times 150 \times 50$ mm and $240 \times 300 \times 50$ mm were cast. The beams were cast along their depths and the panels were cast along their thicknesses (50 mm). The cubes and panels were compacted with a vibrating table, and the beams and cylinders with a 25 mm needle vibrator.

The cylinders were tested after 28 days to determine the compressive strength of the concretes. The flat faces were ground with a diamond disc to ensure uniform loading. The tests were performed under constant displacement rates in a 4.5 MN servo-hydraulic crushing machine with a MTS 458 closed-loop controller.

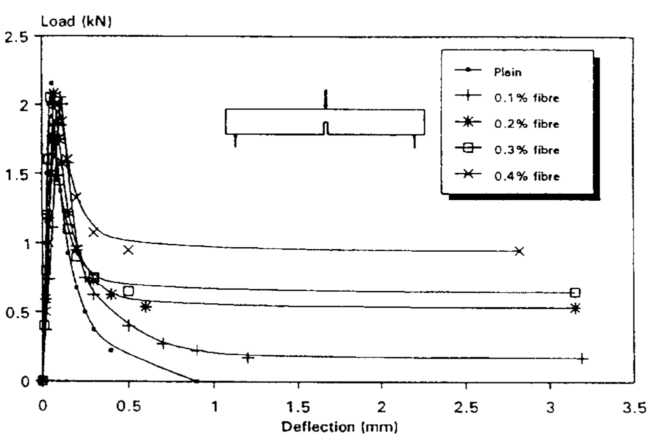

(a)Polypropylene fibre results

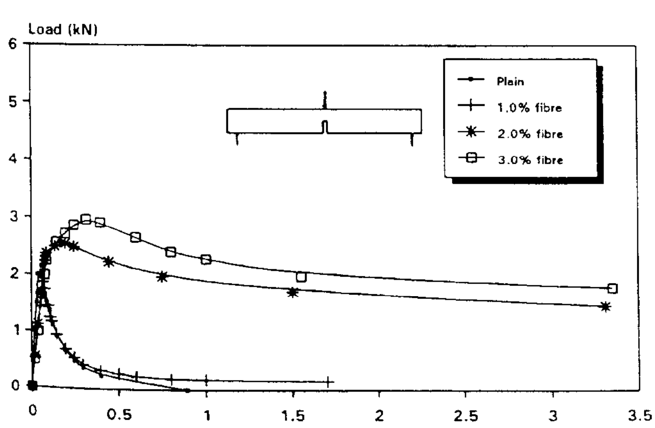

(b)Steel fibre results

Fig. 5. Load–deflection of beams with 50 mm notches; (a) polypropylene fibre concretes and (b) steel fibre concretes.

The strengths obtained for the three concretes are given in Table 3. The post-peak slopes of the load–displacement diagrams indicated the expected increase in ductility with an increase in fibre length. The integrity of the fibre reinforced specimens was maintained even at large displacements while the plain concrete disintegrated just after the peak load. While the plain concrete (HSC-0) failed with the formation of dual cones and vertical splitting cracks, the fibre concrete cylinders failed due to distributed cracking that finally localized along inclined 'shear' planes. This effect was also observed in a qualitative study of the failure of cubes subjected to a punching load. The cubes were loaded, as shown in Fig. 6(a), over the middle-third of the top face and supported over the outer-thirds of the bottom face with steel blocks. Teflon sheets of 0.1 mm thickness were placed between the cube and the bottom supports to minimize the friction due to the transverse deformations. The specimens were loaded under vertical displacement control at a rate of 0.002 mm/s. The objective of these tests was to evaluate the effect of the fibres on concrete subjected to high compressive-shear stresses. The first cracks that occurred in these specimens initiated in the middle-third of the bottom faces at loads of about 130 kN. Since these loads appeared to be unaffected by the presence of the fibres, it was concluded that the initial cracking was produced by the tensile failure of the matrix. This was followed by distributed cracking that appeared in the fibre concretes as inclined bands across the shear planes. Also, the maximum loads for the fibre concretes were higher than for the plain concrete.

The beams were subjected to three-point loading after cutting mid-span notches in them of lengths $a_0 = 0.275d$, where d = beam depth. Note that three sizes of beams were tested in the configuration shown in Fig. 7(a), and they were geometrically similar in two-dimensions (i.e. same thickness but other dimensions proportional to d). The objective was to study the influence of specimen size on the failure behaviour and on the toughening effect of the fibres. The crack opening (CMOD) was measured using an INSTRON clip gage (± 2000 μm range) mounted across the mouth of the notch on 3 mm thick knife-edges. A 100 kN dynamic load cell was used to monitor the load. The tests were controlled to maintain the CMOD

Table 2. Toughness indices based on the load–deflection curve of notched beams

Concrete	V_f (%)		*Notch depth (mm)*	*ASTM C 1018 indices*		*B/3A × 100*
	Steel	*Polypropylene*		I_5	I_{10}	*(%)*
MSC-0.0	0	0	30	2.68	3.47	34.5
			40	2.95	3.67	42.6
			50	2.82	3.71	35.3
MSCP-0.1	0	0.1	30	3.34	4.23	47.2
			40	2.66	3.52	35.3
			50	2.84	3.84	42.7
MSCP-0.2	0	0.2	30	3.14	4.57	44.5
			40	3.10	4.20	42.9
			50	2.72	3.69	35.6
MSCP-0.3	0	0.3	30	2.94	4.77	37.0
			40	3.20	5.20	41.7
			50	2.92	4.31	36.3
MSCP-0.4	0	0.4	30	3.15	5.36	40.4
			40	3.18	5.03	42.4
			50	3.28	5.33	45.3
MSCS-1.0	1	0	30	3.81	6.00	56.9
			40	3.58	5.39	49.9
			50	3.38	5.22	46.0
MSCS-2.0	2	0	30	3.67	6.06	49.4
			40	2.93	4.54	37.2
			50	3.28	5.65	40.4
MSCS-3.0	3	0	30	3.81	6.83	48.7
			40	3.51	6.00	44.4
			50	3.30	5.69	41.2

rates chosen for each size such that the peak loads in the plain concrete specimens occurred at about 3 min. Observations of the failure surfaces indicated that the tortuosity of the crack increased with fibre length. Typical load–CMOD plots for the three concretes are shown in Figs 7(b)–(d). The initial compliance was used to calculate the elastic modulus (E_0) of the concretes.[27] These and other data are given in Table 4. Note that in the HSC-13 specimens, which exhibit hardening-type behaviour after cracking, the first-peak denotes a first well-defined maximum or the bend-over-point.

The panels were used to study the behaviour of the concretes under punching-shear in the configuration shown in Fig. 8(a). The crack propagation in these specimens is non-planar subjecting the fibres to pullout forces that are inclined to the crack faces. As mentioned earlier, the panels were geometrically similar in two-dimensions, with thicknesses of 50 mm. Two notches were cut along the shearing planes

Table 3. Properties of the concretes in series HSC

Concrete	*Superplasticizer content* (l/m^3)	*Slump (in 300 mm cone) (mm)*	*Cylinder compressive strength*		
			Test results (MPa)	*Average (MPa)*	*Coefficient of variation (%)*
HSC-0	12	235	92.7	88.9	3.6
			88.3		
			85.6		
HSC-6	16	260	84.4	87.4	5.9
			90.5		
			87.2		
HSC-13	20	190	87.2	87.3	5.3
			91.0		
			83.8		

of lengths $a_1 = 0.367d$ and $a_2 = 0.3d$. One notch was made longer than the other to ensure crack initiation at its tip so that the opening of this notch could be monitored and used to control the test. Note that even when the notches were

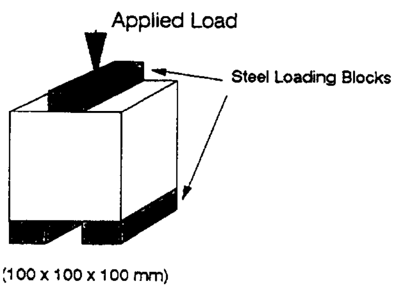

Fig. 6. Loading configuration of the cube specimens

of equal length, it was practically impossible to obtain symmetric crack propagation from both notches. The specimen sides were ground with a diamond disc to avoid non-uniform loading and the loads were applied through rigid steel blocks. Thin Teflon sheets were placed between the specimen and the bottom loading blocks to minimize crack-closing forces due to frictional restraint. The crack opening (CMOD) was measured with a clip gage mounted on knife edges (same as in the beams) placed across the middle of the longer notch, on one face of the panel. The crack sliding (CMSD) was measured using an LVDT (± 5 mm range) mounted, on the other face, with one of its ends fixed to the one edge of the longer notch, at mid-length,

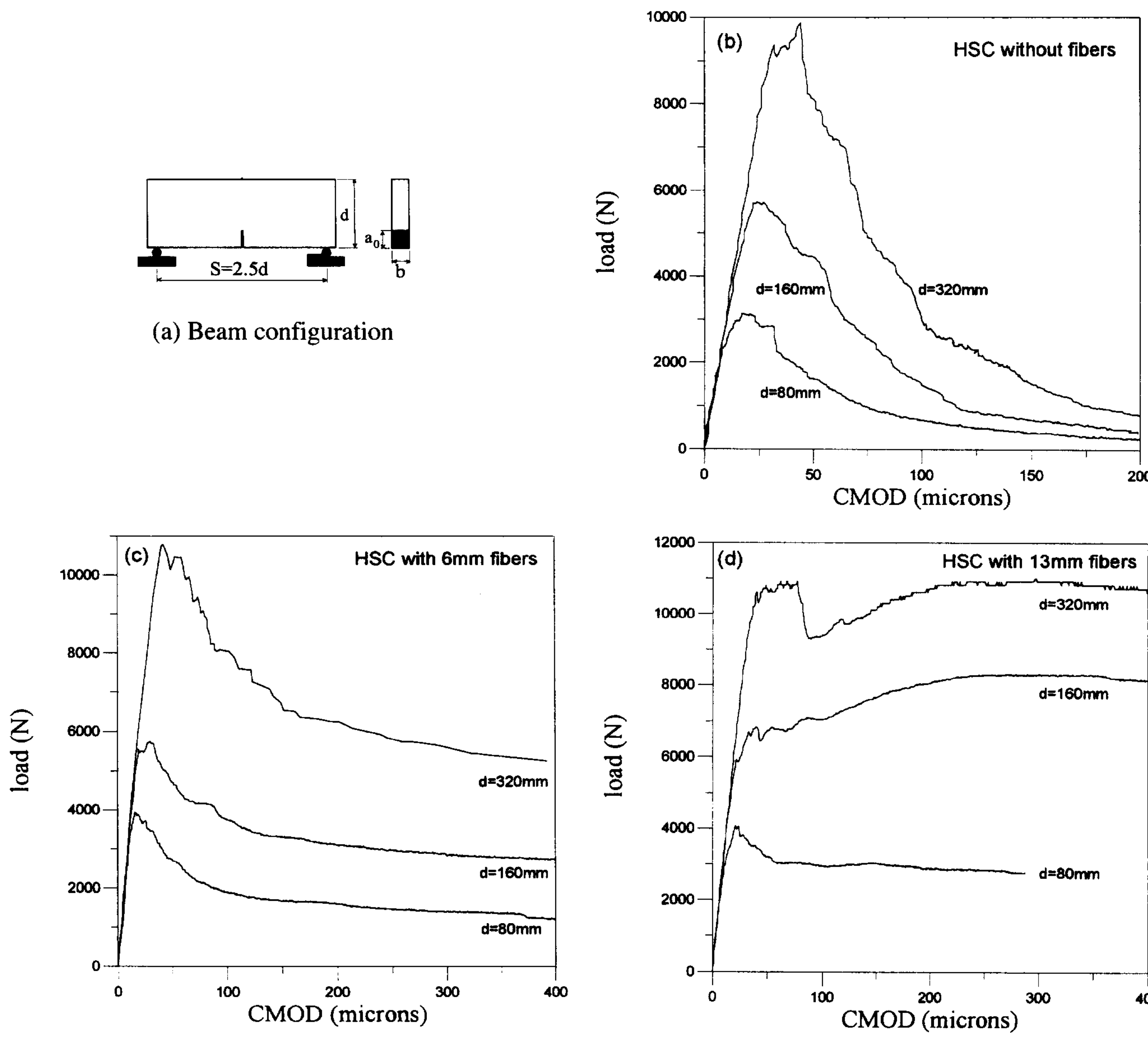

Fig. 7. (a) Configuration of the beams in the HSC series, and typical load–CMOD curves for (b) HSC-0, (c) HSC-6 and (d) HSC-13.

Table 4. Results of notched beam tests of the HSC series

Concrete	Beam depth, d (mm)	CMOD rate (μm/s)	Age at testing (days)	First peak Load (kN)	First peak σ_N (MPa)	First peak CMOD (μm)	E_0 (GPa)
HSC-0	80	0.098	36	3.16	0.790	18	35
			36	3.29	0.823	18	38
			36	3.47	0.868	18	36
	160	0.139	35	5.73	0.716	25	36
			35	6.54	0.818	28	38
			35	6.32	0.790	27	36
	320	0.196	37	10.69	0.668	48	36
			38	9.91	0.619	45	38
HSC-6	80	0.098	34	3.32	0.830	21	32
			35	3.97	0.993	18	36
	160	0.139	33	5.74	0.718	30	36
			33	6.76	0.845	35	36
			33	5.99	0.749	32	36
	320	0.196	36	10.32	0.645	46	36
			36	10.51	0.657	47	38
HSC-13	80	0.098	30	4.02	1.005	24	34
			30	4.10	1.025	23	37
			30	4.10	1.025	24	35
	160	0.139	29	6.80	0.850	40	36
			29	7.00	0.875	48	35
			29	6.35	0.794	40	35
	320	0.196	32	10.60	0.663	48	38
			32	11.39	0.712	66	36
			32	11.33	0.708	56	38

and the other end fixed to the other edge 25 mm away. The tests were controlled to obtain constant CMOD rates, which were chosen to be initially the same as in the beam tests and increased five times after about 6 min (in the post-peak regime). The crack patterns that occurred in the tests are within the scatter bands shown in Fig. 8(b). There was no apparent effect of size on the crack patterns.[21] However, the crack paths are influenced by the fibres. It seems that the crack scatter band decreases with fibre length, and the cracks tend to become straighter and less inclined. Typical load–CMOD curves of the three concretes are shown in Figs 8(c)–(e). The first-peak data in Table 5 show the high scatter in these tests produced mainly by significant variations in the crack path. It was observed that the crack sliding displacement was mainly due to the rotation induced by the curved crack and not due to the shearing of the crack. This can be seen in Fig. 8(f), where the CMOD–CMSD curve is practically linear except initially, confirming the hypothesis that the crack may experience (mixed-mode) opening–sliding displacements at initiation but further propagation occurs with only opening displacements. Furthermore, while the loading configuration suggests punching-shear loading, the failure is governed mainly by tensile cracking.

All specimens were kept in a fog room until testing. The notches were cut with a diamond-edged disc-saw and were about 3 mm wide. All tests on the notched specimens were conducted in a 1 MN INSTRON 8505 servo-hydraulic system with a digital closed-loop controller. Data was acquired electronically using the INSTRON FLAPS software at a frequency of 6 s/point. Further details of the HSC series can be found in Bryars.[28]

Matrix-dominated response of notched specimens

The behaviour of FRC specimens under flexure or tension can be classified in three types, as shown in Fig. 9. Type 1 behaviour is similar to that of plain concrete, with a single peak load followed by softening. Type 2 behaviour is exhibited by FRCs with a small volume fraction of fibres, where the first peak is followed by a drop in load and then a plateau or hardening with a second peak. Type 3 behaviour occurs for higher volume fractions where there is a nonlinear hardening-type response after crack initiation with the absence of softening. In

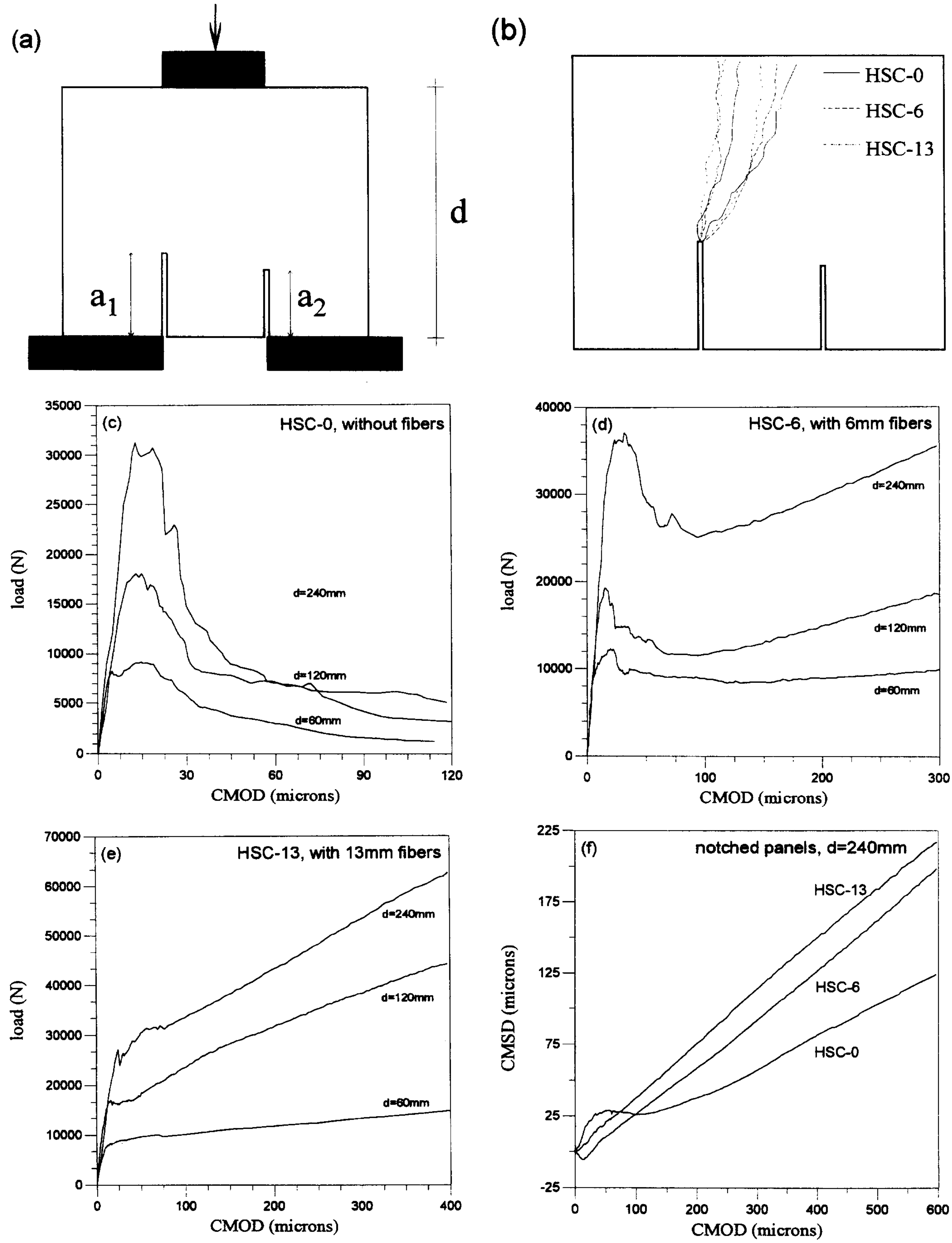

Fig. 8. (a) Configuration of the panel specimens, (b) typical crack bands, typical load–CMOD curves for (c) HSC-0, (d) HSC-6 and (e) HSC-13, and (f) typical CMOD–CMSD curves.

Table 5. Results of panel tests of the HSC series

Concrete	*Panel depth, d (mm)*	*CMOD rate (initial/final) (μm/s)*	*Age at testing (days)*	*First peak*	
				Load (kN)	*CMOD (μm)*
HSC-0	60	0.098/0.393	43	8.96	5
			43	13.05	6
			43	9.17	15
	120	0.139/0.556	42	18.33	12
			42	18.75	9
	240	0.196/0.780	45	33.14	23
			45	41.47	24
			45	32.54	19
HSC-6	60	0.098/0.393	40	13.27	16
			40	12.40	20
			40	13.50	—
	120	0.139/0.556	39	19.65	16
	240	0.196/0.780	42	40.87	32
			42	38.67	28
			42	33.73	25
HSC-13	60	0.098/0.393	35	7.96	9
			35	11.14	16
			35	8.60	8
	120	0.139/0.556	34	13.631	15
			34	7.60	16
			35	12.06	18
	240	0.196/0.780	37	26.40	25
			37	34.46	29
			37	39.76	34

general, the pre-peak behaviour (until the first peak) is practically unaffected by the fibres, as seen in Fig. 3, Fig. 4 and Fig. 5 and Fig. 7 and Fig. 8. It can, therefore, be concluded that this regime is dominated by the matrix and that low volumes of fibres are not very effective before crack initiation. It should be noted that a positive influence of the fibres may be observed in more effective composites, such as HSC-13 that exhibits slightly higher peak loads than HSC-0 and HSC-6, and for very high fibre volumes and continuous fibres.

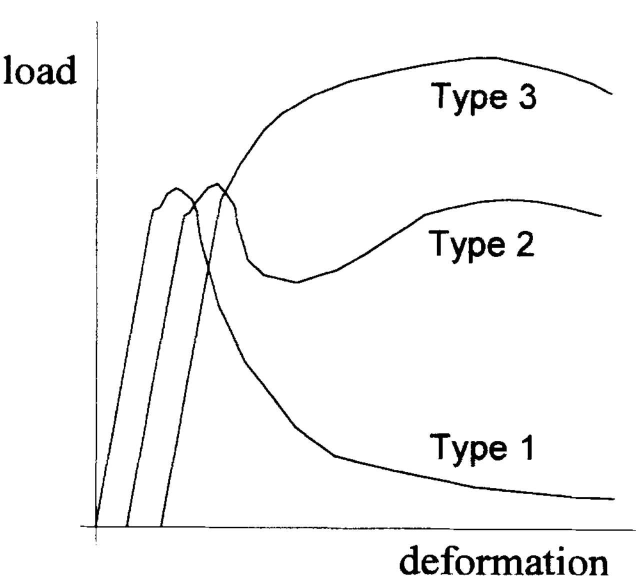

Fig. 9. Classes of load–deformation response observed in FRC.

One important aspect that is confirmed by the pre-peak curves seen in Fig. 3, Fig. 4, Fig. 5 and Fig. 7 and Fig. 8 is the absence of a definite and unambiguous first-crack load, as observed in other works.[4,17,18] As mentioned earlier, to avoid the subjective identification of first-cracking, the first-peak is considered as the end of the matrix-dominated response. It is accordingly proposed that when a reference value is needed for calculating post-cracking toughness in FRC, the first-peak should be used instead of the first-crack, at least in behaviour of Types I and II (Fig. 9).

Another problem with the first-crack or first-peak characteristics is that these values are dependent on the size of the specimen. Consider the first-peak loads shown in Table 3 for the concretes in the HSC series. When these loads are normalized by the beam cross-section area, the nominal maximum stress (σ_N) corresponding to matrix failure is obtained for each specimen. As seen in Table 3, there is a strong size effect on the σ_N-values of the three concretes, where the failure stress decreases with an increase in specimen size. This is an accepted trend in plain concrete and is used in the size effect method of Bazant[23] to determine the fracture parameters (see section 1.2). In earlier work,[20,21,28] this method was applied to the data of HSC-0 and yielded the values of K_{Ic} and c_f as 53.5 MPa-mm$^{0.5}$ and 68 mm, respectively. Similar analyses for HSC-6 and HSC-13 indicated that K_{Ic} (indicating crack resistance of the matrix) decreases slightly due to the addition of fibres and that c_f (indicating the ductility of the matrix) decreases significantly with the increase in fibre length. These trends are interesting but cannot be generalized without further research. Nevertheless, it can be concluded that the use of the pre-peak (including first-peak) behaviour for characterizing FRC can only yield the properties of the matrix-dominated response, except probably in concretes with very low volumes of fibres or with very short fibres.

Toughness based on the load–deflection response of notched beams

As mentioned earlier, the ASTM C 1018 standard[8] defines I_5 as the area under the load–deflection curve up to a deflection of 3 times the first-crack deflection divided by the area up to first-crack, and I_{10} as the area up to a deflection of 5.5 times the first-crack deflection divided by the area up to first-crack (Fig. 1(b)). Another similar index (expressed as a percentage), proposed by Barr and co-workers[5] for both notched and (conventional) unnotched specimens, is the area until twice the first-crack deflection divided by thrice the area until first-crack (B/3A; see Fig. 1(c)). These three indices have been evaluated for the eight concretes in the MSC series, using the areas under the load–deflection curves of the notched beams. The average values obtained are given in Table 2. Note that the peak deflection is used as the reference instead of the first-crack deflection. From the results, it can be seen that the indices calculated for small deflections, such as I_5 (up to thrice the peak value) and B/3A (up to twice the peak value), are not sensitive to the effect of the fibres. The I_{10} index performs slightly better since the deflection limit is 5.5 times the peak deflection. The indices for the plain concrete and some fibre concretes are almost the same, leading to the conclusion that larger deflection limits are needed to obtain more sensitive indices. It is also observed that the notch depth does not have any significant effect on these indices. However, it is always advisable to compare results from specimens with the same geometry to avoid notch sensitivity effects.[25]

Toughness based on the load–CMOD response of notched specimens

The use of the load–CMOD response, instead of load–deflection, to determine toughness has several advantages: (1) CMOD is easier to measure than deflection, (2) CMOD is a direct measure of the deformation across the critical section, that is, the crack plane, and (3) the increase in CMOD is much larger than that of deflection making it more sensitive to the failure. The toughness index used here (TI) is defined as the area under the load–CMOD curve until the CMOD value of $n\delta$ divided by the area until the first-peak, where δ is the CMOD at first-peak and n is a prescribed multiplier (see inset of Fig. 10(b)). The TI-values for notched beams of the HSC series have been computed for different values of n between 2 and 5. The average values and the scatter of the data for the three concretes are shown in Fig. 10(a). It is clear that this index is sensitive to the effectiveness of the fibres and consistently exhibits values that increase with the length of the fibres. Also, there is a strong influence of the CMOD limit on the sensitivity of TI, which increases with an increase in n. To study the influence of specimen size on TI, the data corresponding to $n = 5$ are shown for the three beam depths in Fig. 10(b) and in Table 6. It can be seen that there are no significant effects of specimen dimensions on TI. For all practical purposes, TI seems to be independent of beam size. This implies that the size effect on the peak loads is compensated when the toughness is defined as a ratio of areas. The average values in Table 6 show that TI-values for HSC-6 and HSC-13 are about 1.49 and 1.67 times that of HSC-0.

It should be noted that representative values of toughness are obtained when the specimen dimensions are much larger (at least 3 times) than the fibre length and the maximum aggregate size. Also, the notch width should be much smaller than the fibre length and aggregate size. Though the results indicate that size effects are

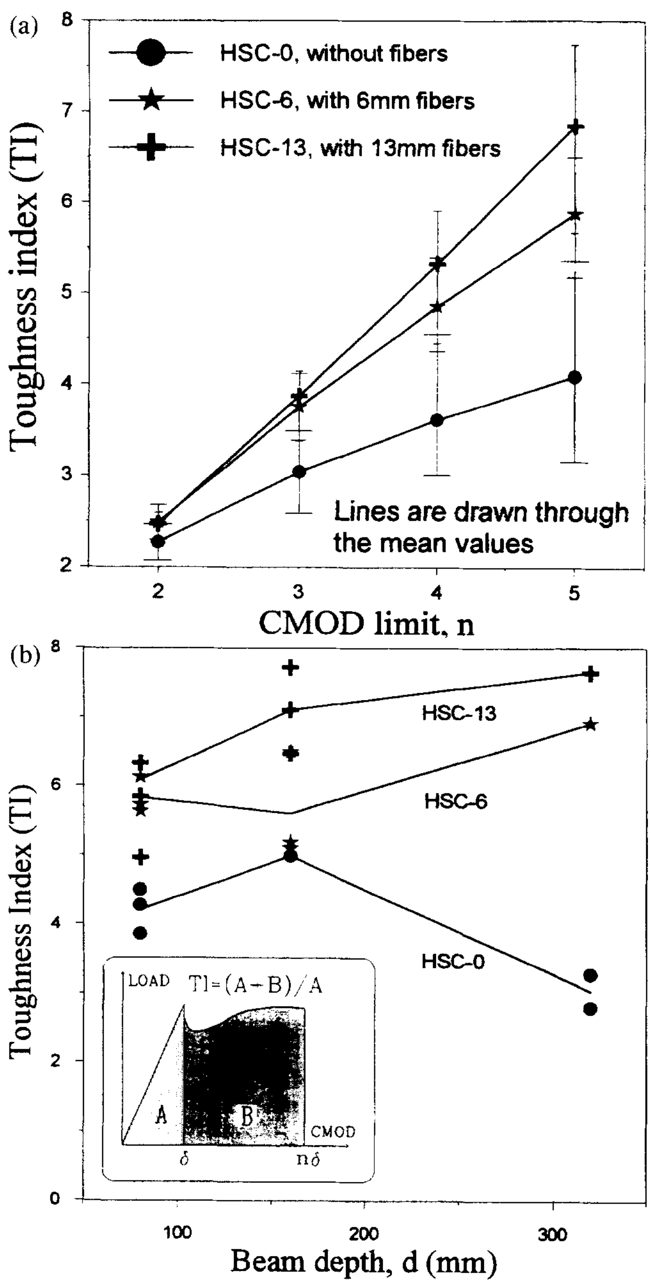

Fig. 10. Toughness indices (TI); influence of (a) the CMOD limit and (b) the specimen size.

negligible it is advisable to compare data from the same specimen geometry and dimensions until more conclusive results are available.

The average TI-values ($n = 5$) for the notched panels, in Table 6, also indicate the increase in toughness with fibre length. Though some results were lost due to problems with the data acquisition system, it was observed that the scatter was much higher, especially in the smaller specimens, than in the beam data. This is mainly attributable to the fact that the crack propagation in the panels is curved and does not follow the notch plane due to the compressive-shear loading. Tests of notched beams avoid this problem and yield more reliable data.

CONCLUSIONS

The first-peak, which signifies matrix failure, is a better and more objective reference value for non-dimensional toughness indices than the first-crack.

The load–CMOD curve is a good basis for defining toughness since CMOD is measured easily and with fewer errors than that observed with traditional toughness measurements based on load–displacement relationships. The load–CMOD curves directly represent the deformation of the critical section. Though this requires more sophisticated testing equipment than that required for load–displacement curves, such testing equipment results in stable post-peak response and avoids the effects of energy dissipation outside the cracking zone.

The CMOD (or deflection) value used as the limit for defining the toughness index should be as large as possible and at least five times that of the peak.

Crack propagation in the notched specimen should be planar and along the notch plane to

Table 6. Toughness indices of the HSC series, for $n = 5$

Concrete	*Average value for each specimen type and size (number of specimens)*							
	Beams				*Panels*			
	small	*medium*	*large*	*all sizes*	*small*	*medium*	*large*	*all sizes*
HSC-0	4.21 (3)	4.99 (1)	3.04 (2)	3.95 (6)	4.37 (3)	5.31 (2)	3.70 (2)	4.45 (7)
HSC-6	5.83 (3)	5.60 (3)	6.91 (1)	5.88 (7)	4.97 (1)	5.46 (1)	5.39 (1)	5.27 (3)
HSC-13	6.09 (3)	7.10 (3)	7.65 (1)	6.58 (7)	—	7.59 (1)	9.69 (2)	8.99 (3)

minimize the variability of the crack path. The specimen dimensions should be much larger than the fibre length (at least thrice) and the maximum aggregate size for obtaining toughness that is representative of the material.

When the test is controlled properly, stable post-peak response is obtained even in plain concrete, contrary to that assumed in several toughness standards. This implies that plain concrete exhibits non-zero toughness, which necessitates the re-definition of the indices that are based on a sudden drop in the load of plain concrete.

ACKNOWLEDGEMENTS

The authors are grateful for support received from Spanish DGICYT Grants PB90-0598, MAT93-0293 and PB93-0955 to the UPC and a Welsh Office Grant to UWCC. Funding for the collaboration between UWCC and UPC was provided by the Acción Integrada Grant 251-B from the British Council and the Spanish Ministry of Education and Science.

REFERENCES

1. Swamy, R. N. & Barr, B. (eds), *Fibre Reinforced Cements and Concretes: Recent Developments*. Elsevier Applied Science, 1989, pp. 700.
2. Swamy, R. N. (ed.), Fibre Reinforced Cement and Concrete, *Proceedings of the Fourth RILEM Interntional Symposium*, E & FN Spon, London, 1992, pp. 1347.
3. National Science Foundation — University of Sheffield Workshop on Fibre Reinfroced Cement and Concrete, Sheffield, U.K., July 1994 (to appear).
4. Gopalaratnam, V. S. & Gettu, R., On the characterisation of flexural toughness in FRC. *Cement & Concrete Composites*, 17 (1995) 239–254.
5. Barr, B. I. G. & Hasso, E. B. D., A Study of Toughness Indicces. *Magazine of Concrete Research*, 37 (1985) 162–173.
6. ACI Committee 544, Measurement of properties of Fiber Reinforced Concrete. *ACI Materials Journal*, 85 (1988) 583–593.
7. Heneger, C. H., Toughness Index of Fibre Concrete, Testing and Test Method of Fibre Cement Composites (RILEM Symposium 1978). Construction Press Ltd., Lancaster, pp. 79–86.
8. ASTM, Standard Test Method for Flexural Toughness and First-Crack Strength of Fiber-Reinforced Concrete (Using Beam with Third-Point Loading), ASTM C 1018-92, *ASTM Annual Book of Standards*, Vol. 04.02, ASTM Philadelphia, U.S.A., 1992, pp. 510–516.
9. Johnston, C. D., Definition and measurement of flexural toughness parameters for fiber reinforced concrete. *Cement, Concrete & Aggregates*, **4** (1982) 53–60.
10. Barr, B. & Liu, K., Fracture of GRC materials. *The International Journal of Cement Composites & Lightweight Concrete*, **4** (1982) 163–171.
11. RILEM Draft Recommendation, 50FMC, Determination of Fracture Energy of Mortar and Concrete by means of three-point bend tests on notched beams. *Materials & Structures*, **18** (1985) 285–290.
12. Hillerborg, A., The theoretical basis of a method to determine the fracture energy G_F of concrete. *Materials & Structures*, **18** (1985) 291–296.
13. RILEM Draft Recommendation, Size effect method for determining fracture energy and process zone size of concrete. *Materials & Structures*, **23** (1990) 461–465.
14. RILEM Draft Recommendation, Determination of fracture parameters (K_{Ic} and $CTOD_c$) of plain concrete using three-point bend tests. *Materials & Structures*, **23** (1990) 457–460.
15. Gopalaratnam, V. S., Shah, S. P., Batson, G. B., Criswell, M. E., Ramakrishnan, V. & Wecharatana, M., Fracture Toughness of Fiber Reinforced Concrete, Report of the Task Group on CMRC/NSF Research, University of Missouri, Columbia, December 1989, 70 pp.
16. Banthia, N., Trottier, J.-F., Wood, D. & Beaupre, D., Steel Fibre reinforced dry-mix shotcrete: Effect of fibre geometry on fibre rebound and mechanical properties. *Fibre Reinforced Cement & Concrete*, ed. R. N. Swamy. E & FN Spon, London, 1992, pp. 277–295.
17. Gopalaratnam, V. S., Shah, S. P., Batson, G. B., Criswell, M. E., Ramakrishnan, V. & Wecharatana, M., Fracture Toughness of Fiber Reinforced Concrete. Report of the Task Group on CMRC/NSF Research, University of Missouri-Columbia, December 1989, pp. 70.
18. Gopalaratnam, V. S., Shah, S. P., Batson, G. B., Criswell, M. E., Ramakrishnan, V. & Wecharatana, M., Fracture Toughness of Fiber Reinforced Concrete. *ACI Materials Journal*, **88** (1991) 339–353.
19. Wang, Y. & Backer, S., Toughness Determination for Fibre Reinforced Concrete. *The International Journal of Cement Composits & Lightweight Concrete*, **11** (1989) 11–19.
20. Bryars, L., Gettu, R., Barr, B. & Aguado, A., Influence of a Low Volume Fraction of Steel Fibers on the Fracture of Silica Fume Concrete, *Anales de Mecánica de la Fractura*, Vol. 11, March 1994, CEIT, San Sebastián, Spain, pp. 318–325.
21. Bryars, L., Gettu, R., Barr, B. & Ari˜no, A., Fracture of Fiber-Reinforced High-Strength Concrete — A Study Based on Size Effect. Fracture and Damage in Quasibrittle Structures, eds Z. P. Bazant, Z. Bittnar, M. Jirásek & J. Mazars. E & FN Spon, London, U.K., 1994, pp. 319–326.
22. Hillerborg, A., Analysis of One Single Crack. In *Fracture Mechanics of Concrete*, ed. F. H. Wittmann. Elsevier Science, Amsterdam, 1983, pp. 223–249.
23. Bazant, Z. P. & Kazemi, M. T., Determination of fracture energy, process zone length and brittleness number from size effect, with application to rock and concrete. *Int. J. of Fracture*, **44** (1991) 111–131.
24. Gettu, R., Prat, P. C. & Kazemi, M. T., Material brittleness from non-linear fracture mechanics. In *Fracture Mechanics of Concrete Structures* (Proc. Int. Conf. FraMCoS1, Breckenridge, USA), ed. Z. P. Bazant. Elsevier Science, London, 1992, pp. 430–436.
25. Gettu, R. & Shah, S. P., Fracture Mechanics. In *High Performance Concretes & Applications*, eds S. P. Shah & S. H. Ahmad. Edward Arnold, London, 1994, pp. 161–212.
26. Al-Oraimi, S. K., Study of Concrete Brittleness, Doctoral Thesis, University of Wales, School of Engineering, Cardiff, U.K., 1993.

27. Gettu, R., Bazant, Z. P. & Karr, M. E., Fracture properties and brittleness of high strength concrete. *ACI Mater. J.*, **87** (1990) 608–618.

28. Bryars, L., Fracture Behaviour of High Performance Concretes, M.Sc. Thesis, University of Wales, School of Engineering, Cardiff, U.K., 1993.